Electronic Supplementary Material (ESI) for Physical Chemistry Chemical Physics.

Supporting Information for: Core-Excited and Shape Resonances of Uracil

Mark A. Fennimore, Spiridoula Matsika*
Department of Chemistry
Temple University
Philadelphia, PA 19122

September 23, 2016

Details of the methodology as well as results are shown here.

1 Methods

1.1 Geometry Optimization

The ground state geometry of uracil was calculated in C1 symmetry using Dunning's standard correlation consistent double-ζ basis set (cc-pVDZ), and the effect of electron correlation was recovered using Møller-Plesset's post Hartree-Fock perturbation theory (MP2). Subsequent vibrational analysis revealed no negative frequencies, indicating that uracil was in a true minimum. Figure 1 shows the optimized geometry of uracil.

1.2 The Stabilization Method: Orbital Scaling

Stabilization curves for the temporary anion states of uracil were generated by evoking the EOM-EA-CCSD method as implemented in QChem 4.2,[1] as well as CASSCF/XMCQDPT2 methods as as implemented in Firefly QC package,[2] which is partially based on the GAMESS (US) source code.[3] All CCSD calculations were performed using frozen 1s orbitals for each of the heteroatoms, and the system was constrained to Cs symmetry. The CASSCF calculations too were performed in Cs symmetry and the complete active space (CAS) was assigned carefully as to capture the shape and core-excited resonances of interest. Cs symmetry significantly increased convergence of the EOM/CASSCF matrix and aided with the analysis of the stabilization curves. This latter point is important because states of dissimilar Irreps (i.e. A' and A'') do not interact with one another; and as such, avoided crossings and, therefore, widths can only be obtained between states of similar symmetry.

Furthermore, because standard basis sets are not able to properly differentiate true resonance states from orthogonal discretized continuum (ODC) solutions, non-standard basis

---

*Email address: smatsika@temple.edu

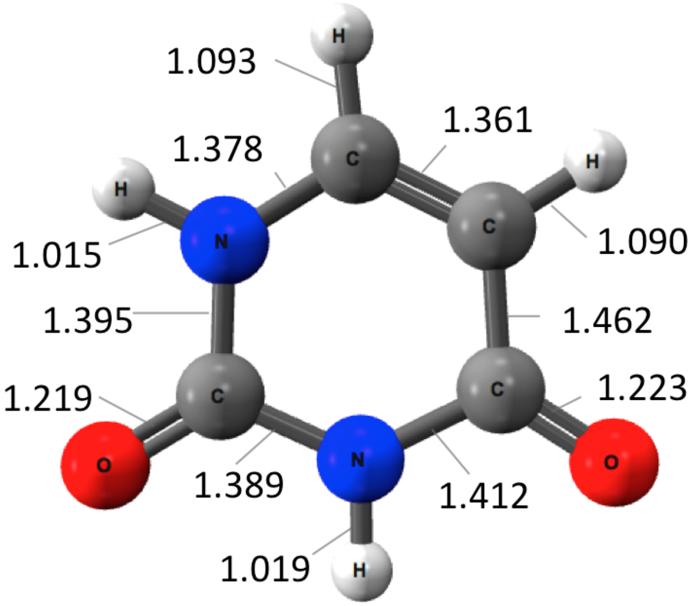

Figure 1: Optimized geometry of uracil at the MP2/cc-pVDZ level. Bond lengths are shown in Å. The geometry is planar. This geometry was used in all subsequent calculations. IQMol 2.7 was used for visualization.

sets were used to construct the so called resonance stabilization curves.[4,5] The resonance stabilization curves presented in this work were generated by scaling the diffuse functions on Pople's 6-31+G(d), 6-311+G(d) and Dunning's aug-cc-pVDZ basis sets. The diffuse functions were adjusted by introducing a scaling parameter (α), which at low values (e.g. 0.1) correspond to highly diffuse atomic orbitals, and at large values (e.g. 2.0) correspond to less diffuse, more contracted atomic orbitals. The real resonance solutions using the stabilization method are those solutions whose energy is invariant with respect to α.[6] The scaling of diffuse functions may be conveniently expressed as 6-31(α)+ G(d), 6-311(α)+ G(d) and (α)aug-cc-pVDZ. In the case of the Pople basis sets, α is used only to scale the diffuse functions on the heteroatoms (N, C and O), while for the Dunning basis set, α scales the diffuse function on each hydrogen as well as the heteroatoms. Note that scaling $\alpha = 1$ corresponds to the default diffuse orbital exponent for a given standard basis set. The default ($\alpha = 1$) 6-31+G(d) and 6-311+G(d) diffuse orbital exponents for C(SP), N(SP) and O(SP) are 0.0438, 0.0639 and 0.0845 respectively. These were all scaled uniformly from α=0.15 to 2.4 with $\Delta\alpha$=0.05. Also worthy of note is that the augmented Dunning double-ζ basis set contains diffuse functions for both the s-orbitals as well as the p and d-orbitals. These too were scaled homogenously. Their default ($\alpha = 1$) values were H(S)=0.02974, C(S)=0.0469, N(S)=0.06124, O(S)=0.07896, H(P)=0.0141, C(P)=0.04041, N(P)=0.05611, O(P)=0.06656, C(D)=0.1510, N(D)=0.2300 and O(D)=0.3320, where the S, P and D following the element symbol is indicative of the orbital type according to the Gaussian 94 style of notation. The aug-cc-pvdz+1s,1p,1d basis set was created by adding three additional diffuse functions on each heteroatom (1s,1p and 1d) with an exponent half the value of the exponent in the original diffuse functions.

1.3 Orbitals involved in CASSCF/XMCQDPT2

The CASSCF calculations consisted of 5 occupied π (25-29) and 4 virtual π^* (30-33) orbitals. One diffuse π^* orbital was included in the active space to promote the formation of ODC solutions, which can interact with the π^* resonance states resulting in avoided crossings. These avoided crossings were then used to calculate the resonance parameters E_r and Γ. The calculations were based on an average of 7 A'' states. The orbitals involved in the active space are shown in Figure 2.

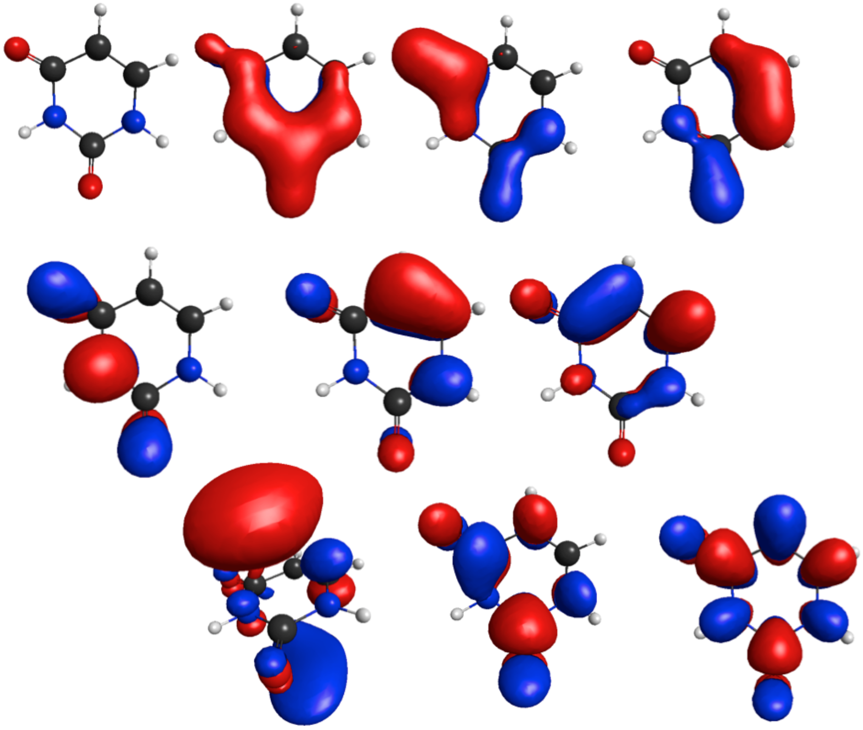

Figure 2: Orbitals included in the CASSCF active space

1.4 Analysis of Stabilized Curves: the General Padé Approximation (GPA)

Analytic Continuation (AC) can be used with the orbital stabilization method (discussed in Section 1.2), where the complex branch points and energies are located using various forms of the Generalized Padé Approximation (GPA). The method is decribed in the main text, while some additional details are given here. In the present work, the data points from the upper and lower roots used to determine the resonance parameters via AC were centered at the point of nearest approach (α_{na}) at the avoided crossing. In the case of the (4,4,4) GPA, there are an equal and symmetric number of data points centered at α_{na}; however, with all other approximations, an additional data point is required. Therefore, as a matter of convention, the additional point was assigned from the lower root at increased α, as per Figure 3.

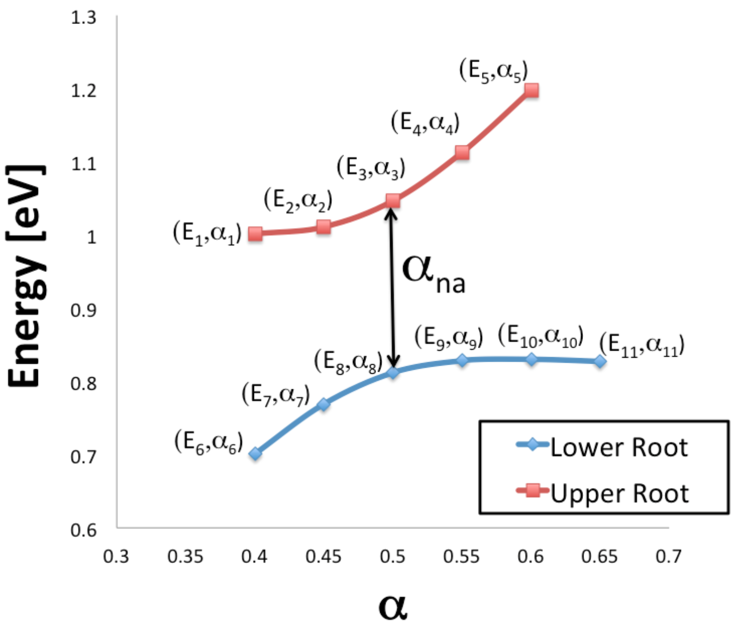

Figure 3: Analysis of an avoided crossing via the GPA begins with assigning the values for the upper and lower roots to be used in AC. With these values, a matrix is constructed to solve the set of linear equations for the coefficients p_i, r_k, q_j and s_l.

$$\begin{bmatrix} E_1^2\alpha_1 & E_1^2\alpha_1^2 & E_1^2\alpha_1^3 & E_1 & E_1\alpha_1 & E_1\alpha_1^2 & E_1\alpha_1^3 & 1 & \alpha_1 & \alpha_1^2 & \alpha_1^3 \\ E_2^2\alpha_2 & E_2^2\alpha_2^2 & & & & & & & & \alpha_2^2 & \alpha_2^3 \\ E_3^2\alpha_3 & & & & & & & & & & \alpha_3^3 \\ & & & & & & & & & & \\ . & & & & & & & & & & . \\ . & & & & & & & & & & . \\ . & & & & & & & & & & . \\ & & & & & & & & & & \\ E_9^2\alpha_9 & & & & & & & & & & \alpha_9^3 \\ E_{10}^2\alpha_{10} & E_{10}^2\alpha_{10}^2 & & & & & & & & \alpha_{10}^2 & \alpha_{10}^3 \\ E_{11}^2\alpha_{11} & E_{11}^2\alpha_{11}^2 & E_{11}^2\alpha_{11}^3 & E_{11} & E_{11}\alpha_{11} & E_{11}\alpha_{11}^2 & E_{11}\alpha_{11}^3 & 1 & \alpha_{11} & \alpha_{11}^2 & \alpha_{11}^3 \end{bmatrix} \begin{bmatrix} p_1 \\ p_2 \\ p_3 \\ s_0 \\ s_1 \\ s_2 \\ s_3 \\ r_0 \\ r_1 \\ r_2 \\ r_3 \end{bmatrix} = \begin{bmatrix} E_1^2 \\ E_2^2 \\ E_3^2 \\ E_4^2 \\ E_5^2 \\ E_6^2 \\ E_7^2 \\ E_8^2 \\ E_9^2 \\ E_{10}^2 \\ E_{11}^2 \end{bmatrix}$$

Figure 4: The system of equations generated using the, in this case, (3,3,3) GPA. The subscripts here (i.e. 1-11) indicate which particular value of E and α were used from the resonance stabilized curves as per Figure 3.

The use of analytic continuation to determine the location of complex stationary points in α can routinely give rise to spurious solutions; therefore, to test the validity of a given result, each avoided crossing was subjected to analysis using multiple forms of the GPA, i.e. various forms of (n_i, n_j, n_k) and (n_i, n_j, n_k, n_l). The "true" resonance solutions are considered those which are consistent across multiple methods. Higher order GPA's, e.g. (4,4,4,4) and (5,5,5,5), were deemed unnecessary for the present work due to the high level of consistency obtained with lower order approximations.

2 Results and Discussion

2.1 EOM-EA-CCSD on Singlet Uracil

For each of the basis sets examined, the A'' shape resonances were determined via analysis of the avoided crossings using the analytic continuation procedure outlined in Section 1.4. The stabilization curves generated are shown below. Figure 5 shows the stabilization curves obtained from EOM-EA-CCSD on the singlet ground state of uracil using the 6-31+G(d), 6-311+G(d) and aug-cc-pVDZ basis sets. The stabilization curves at the aug-cc-pVDZ+1s,1p,1d are shown in the main manuscript. Only A'' symmetry states are included in the calculations in order to obtain couplings between ODC and resonances. The presence of 3 A'' resonance states for all basis sets is strongly suggested by the stabilization curves. These resonance states were later confirmed through Analytic Continuation onto the complex plane via the (3,3,3), (4,4,4), (5,5,5) and (3,3,3,3) GPA. For each stabilization graph, there were one, two and four avoided crossing used to characterize the resonance energy for the $1A''$, $2A''$ and $3A''$ shape resonances, respectively. In the case of the $2A''$ resonance, additional avoided crossings were present at low values of α; however, these avoided crossings tended to give rise to errors in the analytic continuation procedure and were, therefore, not included. Regarding the third A'' shape resonance, multiple avoided crossings, with strongly varying degrees of coupling, are clearly present.

Tables 1, 2, 3 summarize the results for the resonances found from the stabilization curves via Analytic Continuation. The results obtained from the (3,3,3), (4,4,4), (5,5,5) and (3,3,3,3) approaches yield very similar results. The results obtained from different avoided crossings show larger variations, indicative of the uncertainty in this approach.

Table 1: Complex energies of the first three A'' shape resonances associated with Analytic Continuation using the EOM-EA-CCSD/6-31+G(d) stabilization graph (Figure 5 (top panel)). Results for each avoided crossing (X i) are shown.

	GPA	$1\pi^*$ E_r (Γ) [eV]	$2\pi^*$ E_r (Γ) [eV]	$3\pi^*$ E_r (Γ) [eV]
X 1	(3,3,3)	1.0320 (0.0752)	2.6608 (0.203)	5.6414 (0.0697)
	(4,4,4)	1.0312 (0.0758)	2.6583 (0.2019)	5.6416 (0.0669)
	(5,5,5)	1.0313 (0.0756)	2.658 (0.2021)	5.6454 (0.0659)
	(3,3,3,3)	1.0308 (0.0766)	2.6597(0.1998)	5.6414 (0.0674)
X 2	(3,3,3)		2.4466 (0.3065)	5.8411 (0.0872)
	(4,4,4)		2.4540 (0.2982)	5.8413 (0.0866)
	(5,5,5)		2.4531 (0.2968)	5.8410 (0.0865)
	(3,3,3,3)		2.4513 (0.2966)	-
X 3	(3,3,3)			5.7868 (0.6717)
	(4,4,4)			5.7858 (0.6761)
	(5,5,5)			5.7857 (0.6589)
	(3,3,3,3)			5.7868(0.6634)
X 4	(3,3,3)			5.2774 (0.2246)
	(4,4,4)			5.2765 (0.2230)
	(5,5,5)			5.2761 (0.2159)
	(3,3,3,3)			5.2921 (0.2032)

Table 2: Complex energies of the first three A'' shape resonances associated with Analytic Continuation using the EOM-EA-CCSD/6-311+G(d) stabilization graph (Figure 5 (middle panel)). Results for each avoided crossing (X i) are shown.

	GPA	$1\pi^*$ E_r (Γ) [eV]	$2\pi^*$ E_r (Γ) [eV]	$3\pi^*$ E_r (Γ) [eV]
X 1	(3,3,3)	0.9108 (0.0732)	2.5408 (0.2014)	5.4606 (0.0336)
	(4,4,4)	0.9107 (0.0732)	2.5321 (0.1887)	5.4611 (0.0298)
	(5,5,5)	0.9101 (0.0732)	2.5323 (0.1888)	5.4681 (0.0376)
	(3,3,3,3)	0.9108 (0.0732)	2.5346 (0.1886)	5.4617 (0.0279)
X 2	(3,3,3)		2.3458 (0.2965)	5.6304 (0.0879)
	(4,4,4)		2.3419 (0.2998)	5.6307 (0.0883)
	(5,5,5)		2.3362 (0.2853)	5.6360 (0.0847)
	(3,3,3,3)		2.3442 (0.3012)	5.6308 (0.0881)
X 3	(3,3,3)			5.6455 (0.5951)
	(4,4,4)			5.6453 (0.593)
	(5,5,5)			5.6464 (0.5875)
	(3,3,3,3)			5.6483 (0.5894)
X 4	(3,3,3)			5.1660 (0.3177)
	(4,4,4)			5.1663(0.3207)
	(5,5,5)			5.1733 (0.3133)
	(3,3,3,3)			5.1656 (0.3165)

Table 3: Complex energies of the first three A'' shape resonances associated with Analytic Continuation using the EOM-EA-CCSD/aug-cc-pVDZ stabilization graph (Figure 5 (bottom panel)). Results for each avoided crossing (X i) are shown.

	GPA	$1\pi^*$ E_r (Γ) [eV]	$2\pi^*$ E_r (Γ) [eV]	$3\pi^*$ E_r (Γ) [eV]
X 1	(3,3,3)	0.7262 (0.0915)	2.3816 (0.1617)	4.8238 (0.1165)
	(4,4,4)	0.7281 (0.0923)	2.3817 (0.1606)	4.8262 (0.1159)
	(5,5,5)	0.7282 (0.0925)	2.3815 (0.1614)	4.8265 (0.1162)
	(3,3,3,3)	0.7277 (0.0887)	2.3795 (0.1579)	4.8249 (0.1166)
X 2	(3,3,3)		2.2406 (0.2880)	5.2687 (0.1428)
	(4,4,4)		2.2539 (0.2795)	5.2687 (0.1428)
	(5,5,5)		2.2608 (0.2824)	5.2802 (0.1433)
	(3,3,3,3)		2.2503 (0.2890)	5.2688 (0.1424)
X 3	(3,3,3)			5.2634 (0.6089)
	(4,4,4)			5.2676 (0.6077)
	(5,5,5)			5.2997 (0.5659)
	(3,3,3,3)			5.2812 (0.6079)
X 4	(3,3,3)			4.9359 (0.2606)
	(4,4,4)			4.9367 (0.2585)
	(5,5,5)			-
	(3,3,3,3)			4.9343 (0.2584)

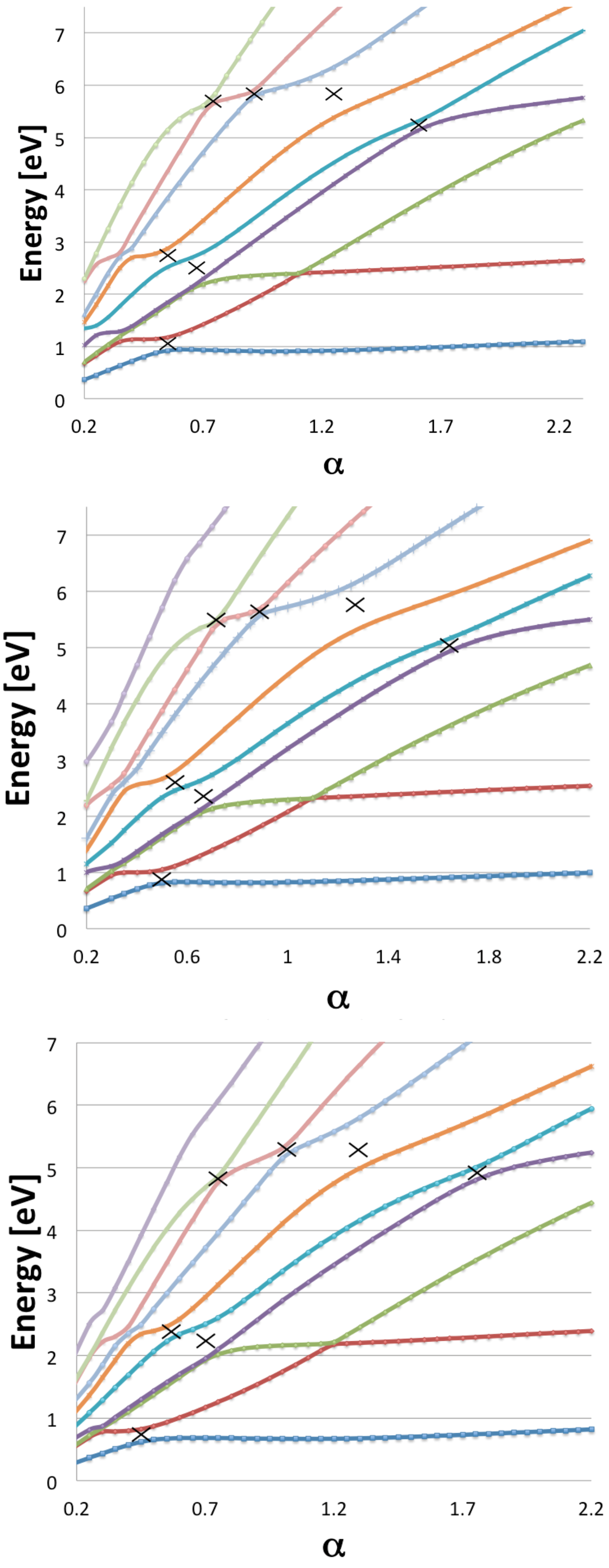

Figure 5: Stabilization curves associated with the (top) EOM-EA-CCSD/6-31+G(d); (middle) EOM-EA-CCSD/6-311+G(d); (bottom) EOM-EA-CCSD/aug-cc-pVDZ method. The singlet ground state of uracil is the reference. The location of each avoided crossing used in the Analytic Continuation is highlighted with an “X”

Table 4: $\pi^1(\pi^*)^2$ core-excited resonance energies and widths (in parenthesis) in eV for the 6-31+G(d), 6-311+G(d), aug-cc-pVDZ and aug-cc-pVDZ+1s,1p,1d scaled basis functions.

GPA	6-31+G(d)	6-311+G(d)	aug-cc-pVDZ	aug-cc-pVDZ+1s,1p,1d
(3,3,3)	5.6559 (0.1512)	5.5541 (0.1513)	5.3164 (0.1328)	5.2888 (0.1455)
(4,4,4)	5.6559 (0.1512)	5.5545 (0.1512)	5.3166 (0.1327)	5.2884 (0.1473)
(5,5,5)	5.6557 (0.1511)	5.5542 (0.1512)	5.3177 (0.1322)	-
(3,3,3,3)	5.6561 (0.1512)	5.5541 (0.1512)	5.3166 (0.1327)	5.2969 (0.1481)

Table 5: $n^1(\pi^*)^2$ core-excited resonance energies and widths (in parenthesis) in eV for the 6-31+G(d) and 6-311+G(d) basis functions.

GPA	6-31+G(d)	6-311+G(d)
(3,3,3)	6.4905 (0.1211)	6.2672 (0.1183)
(4,4,4)	6.4937 (0.1186)	6.2668 (0.1177)
(5,5,5)	6.4941 (0.1189)	6.2666 (0.1158)
(3,3,3,3)	6.4940 (0.1195)	6.2670 (0.1174)

2.2 EOM-EA-CCSD on Triplet Uracil

Figures 6, 7, 8 show the stabilization curves obtained using EOM-EA-CCSD when the reference is the triplet $\pi^1(\pi^*)^1$ state. Even though more than one resonance appears, we only focus on the core-excited $\pi^1(\pi^*)^2$ one. The lowest state in this calculation corresponds to the lowest shape resonance of uracil, since the lowest energy addition of an electron to the triplet $\pi^1(\pi^*)^1$ state leads to $(\pi)^2(\pi^*)^1$. This resonance is a stable state with positive EA when the reference is the triplet state.

Figure 9 shows the stabilization curve obtained using EOM-EA-CCSD when the reference is the triplet $n^1(\pi^*)^1$ state. Again, we only focus on the $n^1(\pi^*)^2$ resonance. In this calculation we could not obtain separately the A' and A'' states so there are many states that are not coupled. We used only one pair of states that were coupled to each other to extract the complex energy. We had difficulties obtaining the aug-cc-pVDZ curves for this reference, so we only report 6-31+G(d) and 6-311+G(d) results. Based in the fact that we do not see great dependence of the complex energies on the basis set we do not expect this to be a problem, and we report the 6-311+G(d) results as our best estimate.

Tables 4 and 5 summarize the results obtained from the avoided crossings in the stabilization curves for the triplet states. There is only one avoided crossing for each plot. The results again are very stable with respect to different GPA expansions. Equation 1 illustrates how the adjusted singlet and triplet resonance positions were derived so that all resonances have the same reference. The last term is the difference between the singlet and triplet CCSD ground state energy at the avoided crossing as illustrated in Figure 10.

$$E_r^{adj} = E_\alpha^{State_i} + \Delta E_\alpha^{S_0-T_0} \tag{1}$$

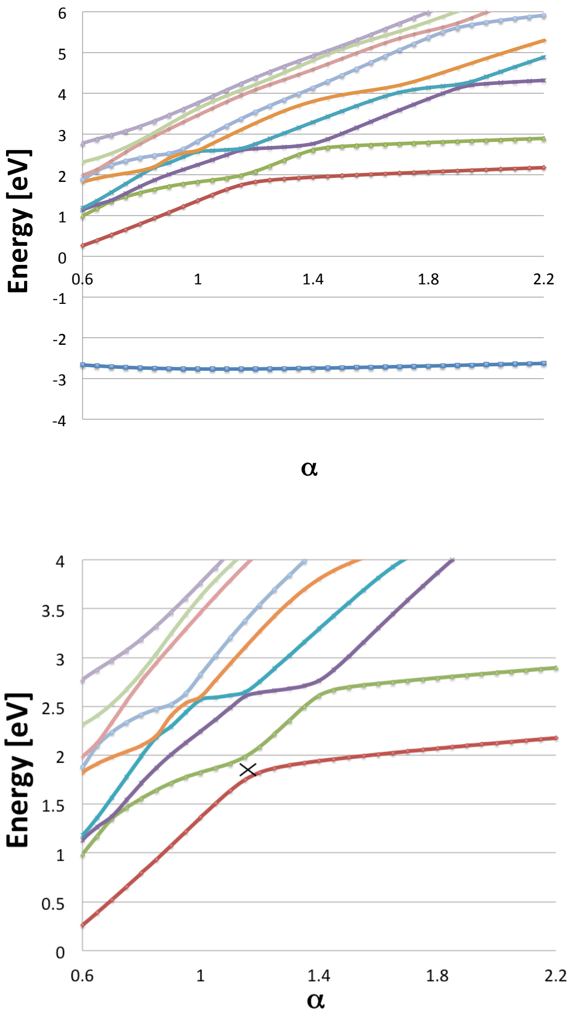

Figure 6: Stabilization curves associated with $\pi^1(\pi^*)^1$ triplet uracil at the EOM-EA-CCSD/6-31+G(d) level of theory. Top plot shows all the states, while the bottom plot focuses on the avoided crossing used in this work.

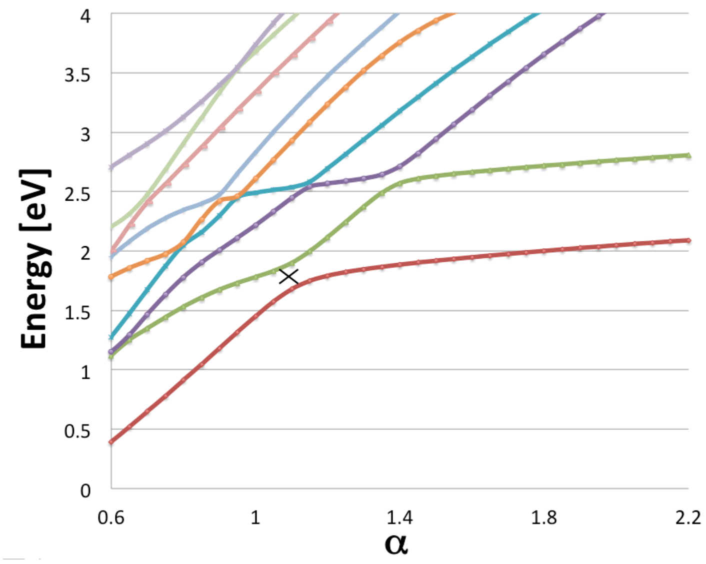

Figure 7: Stabilization curves associated with $\pi^1(\pi^*)^1$ triplet uracil at the EOM-EA-CCSD/6-311+G(d) level of theory.

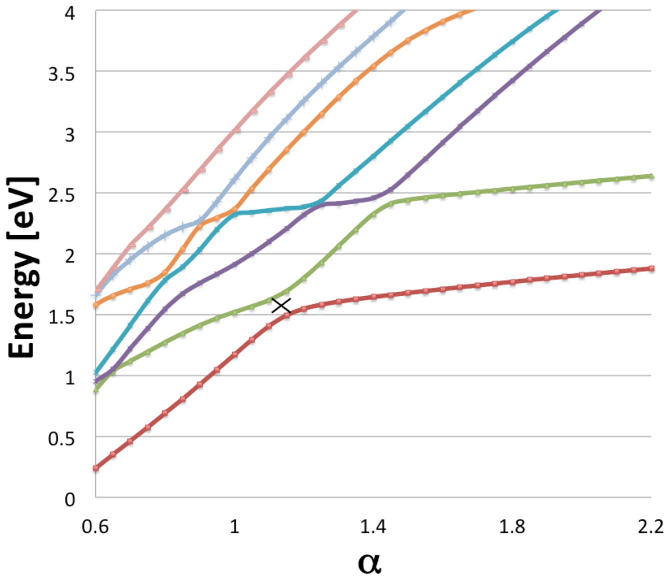

Figure 8: Stabilization curves associated with $\pi^1(\pi^*)^1$ triplet uracil at the EOM-EA-CCSD/aug-cc-pVDZ level of theory.

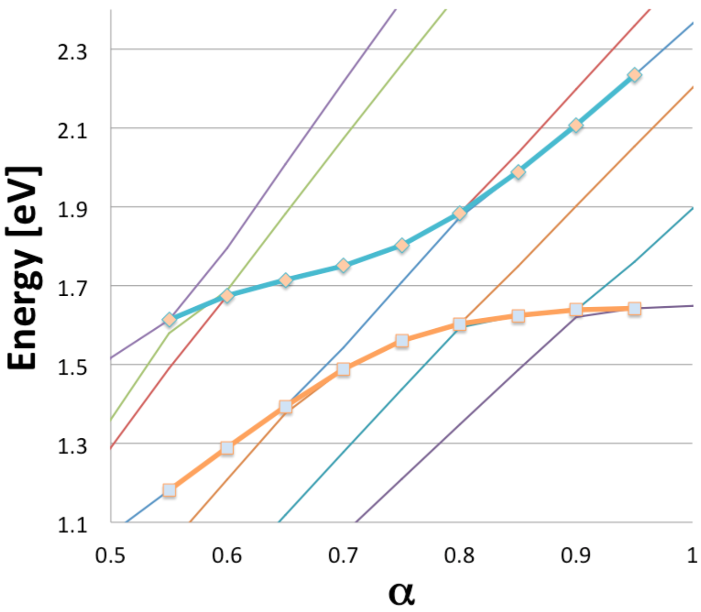

Figure 9: Stabilization curves associated with $n^1(\pi^*)^1$ triplet uracil at the EOM-EA-CCSD/6-31+G(d) level of theory.

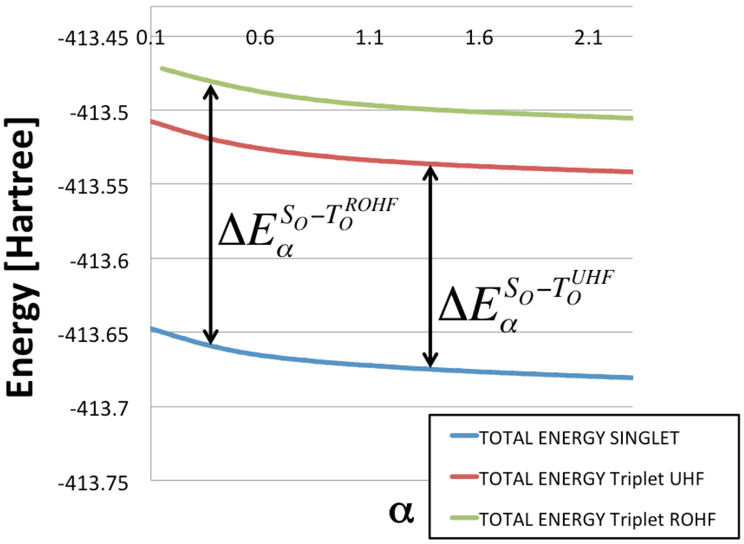

Figure 10: Singlet and triplet coupled cluster ground state energies as a function of the scaled aug-cc-pVDZ basis set. The difference between these two states, at the point of an avoiding crossing, was used to adjust the triplet EOM-EA-CCSD states relative to singlet configuration.

Table 6: Energies and widths obtained at the CASSCF/6-31+G(d) and XMCQDPT2/6-31+G(d) levels. The energy of the first resonance has been shifted to the experimental value of 0.22 eV

		CASSCF	MCQDPT
	GPA	E_r (Γ) [eV]	E_r (Γ) [eV]
$1\pi^*$	(3,3,3)	0.22 (0.1207)	0.22 (0.0043)
	(4,4,4)	0.22 (0.1201)	0.22 (0.0038)
	(5,5,5)	0.22 (0.1207)	0.22 (0.0061)
	(3,3,3,3)	0.22 (0.1208)	0.22 (0.0035)
$2\pi^*$	(3,3,3)	1.8993 (0.0506)	1.1863 (0.0156)
	(4,4,4)	1.8994 (0.0537)	1.1865 (0.0157)
	(5,5,5)	-	1.1861 (0.0172)
	(3,3,3,3)	1.9455 (0.0804)	1.1865 (0.0157)
$3\pi^* + \pi^1(\pi^*)^2$	(3,3,3)	4.8589 (0.0961)	4.1756 (0.0105)
	(4,4,4)	4.8562 (0.0936)	4.1775 (0.0102)
	(5,5,5)	4.8689 (0.0875)	4.1749 (0.0114)
	(3,3,3,3)	4.8761 (0.1258)	4.1756 (0.0119)
$\pi^1(\pi^*)^2 + 3\pi^*$	(3,3,3)	5.5981 (0.2331)	4.5561 (0.0883)
	(4,4,4)	5.5621 (0.2869)	4.5551 (0.0876)
	(5,5,5)	5.625 (0.2987)	4.5546 (0.0876)
	(3,3,3,3)	5.6999 (0.2631)	4.5571 (0.0850)

2.3 CASCSF and XMCQDPT2

The stabilization curves obtained using CASSCF and XMCQDOT2 are shown in the main manuscript. The complex energies obtained from the avoided crossings in this graph are shown in Table 6.

References

[1] Shao, Y.; Fusti-Molnar, L.; Jung, Y.; Kussmann, J.; Ochsenfeld, C.; Brown, S. T.; Gilbert, A. T. B.; Slipchenko, L. V.; Levchenko, S. V.; O'Neill, D. P.; Jr., R. A. D.; Lochan, R. C.; Wang, T.; Beran, G. J. O.; Besley, N. A.; Herbert, J. M.; Lin, C. Y.; Voorhis, T. V.; Chien, S. H.; Sodt, A.; Steele, R. P.; Rassolov, V. A.; Maslen, P. E.; Korambath, P. P.; Adamson, R. D.; Austin, B.; Baker, J.; Byrd, E. F. C.; Daschel, H.; Doerksen, R. J.; Dreuw, A.; Dunietz, B. D.; Dutoi, A. D.; Furlani, T. R.; Gwaltney, S. R.; Heyden, A.; Hirata, S.; Hsu, C.; Kedziora, G.; Khaliullin, R. Z.; Klunzinger, P.; Lee, A. M.; Lee, M. S.; Liang, W. Z.; Lotan, I.; Nair, N.; Peters, B.; Proynov, E. I.; Pieniazek, P. A.; Rhee, Y. M.; Ritchie, J.; Rosta, E.; Sherrill, C. D.; Simmonett, A. C.; Subotnik, J. E.; III, H. L. W.; Zhang, W.; Bell, A. T.; Chakraborty, A. K.; Chipman, D. M.; Keil, F. J.; Warshel, A.; Hehre, W. J.; III, H. F. S.; Kong, J.; Krylov, A. I.; Gill, P. M.; Head-Gordon, M. *Phys. Chem. Chem. Phys.* **2006**, *8*, 3172.

[2] Firefly version 8, www http://classic.chem.msu.su/gran/firefly/index.html. Granovsky, A. A.

[3] Schmidt, M. W.; Baldridge, K. K.; Boatz, J. A.; Elbert, S. T.; Gordon, M. S.; Jensen, J. H.; Koseki, S.; Matsunaga, N.; Nguyen, K. A.; Su, S.; Windus, T. L.; Dupuis, M.; Montgomery, J. A. *J. Comput. Chem.* **1993**, *14*, 1347.

[4] Hazi, A. U.; Taylor, H. S. *Phys. Rev. A* **1970**, *1*, 1109.

[5] Simons, J. *J. Chem. Phys.* **1981**, *75*, 2465.

[6] Moiseyev, N.; Certain, P. R.; Weinhold, F. *Mol. Phys.* **1978**, *36*, 1613.